

Meteorologisches Institut, Universität Hamburg, Germany

## Response of Tropical Convective Complexes to Primary Circulation Induced Heating

K. Fraedrich

With 3 Figures

Received January 23, 1998

Revised April 28, 1998

### Summary

The instability due to cumulus heating in the inner region of a balanced slab-symmetric two-layer model with an underlying Ekman layer is analysed. In satisfying the water balance the heating comprises two terms: One can be associated with the wind-evaporation feedback (representing a WISHE-type\* parameterisation) and replaces the CISK-type heating originally employed in the classical Charney-Eliassen model. The second is associated with the mid-level vertical mass flux. The model comprises two regimes of instability depending on the scale and the dominance of either one of the heating terms: (i) Dominance of the WISHE-type heating is characterised by hyperbolic meridional eigenfunctions, which represent the spatial structure of the inner region. It requires sufficient intensity of the surface heat exchange to obtain finite growth rates within a finite scale range. Beyond a certain threshold of the heating parameter the unstable scale range extends to infinitely large values. The maximum growth rates, though relatively small, occur at the smaller scale limit, which separates both regimes. (ii) Dominance of the mid-level term requires trigonometric meridional eigenfunctions to represent the spatial structure of the inner region; the growth rates range from zero to infinity associated with a finite range of spatial scales. It joins the other regime at its large growth (and small scale) boundary. In this linear model the influence of wind induced surface heat exchange tends to enlarge the spectrum of spatial scales effected by the heating induced instability.

### 1. Introduction

Riehl, in 1954, emphasized the importance of heat fluxes from the sea in the genesis of tropical storms. In an early modelling attempt, Charney and Eliassen (1964) introduced a *linear* dynamical system to describe the response of the large scale flow of a tropical *f*-plane atmosphere on cumulus heating induced by Ekman pumping. The implicate assumption of an infinite (sea surface heat and moisture) reservoir is a common feature of linear modelling. The resulting instability shows two modes of behaviour. The fast mode has been rejected (growing with infinitely fast rate at *finite* horizontal scale) non-physical while the slow mode (growing with finite, though relatively slow, maximum rates at *zero* scale) has been coined CISK (conditional instability of the second kind). This instability seems to be losing favour as a suitable theory for the genesis of tropical disturbances, although the dynamical feedback mechanism and the appropriate water balance involved have not been described until rather recently. One of the reasons is that *non-linear* dynamical systems are being advocated to describe the large scale flow response on a cumulus heating parameterised by a wind induced surface heat exchange (WISHE, after Yano and Emanuel, 1991).

\* WISHE = Wind Induced Surface Heat Exchange.

A WISHE-type heating instead of a CISK parameterisation is used to drive a Charney-Eliassen type model and to interpret the instability in terms of Ooyama's (1997) review on 'cooperative intensification and maintenance theory' of tropical systems, the participants of this cooperation being the primary and the secondary circulation. The model's moisture budget requires a mid-level heating which depends on the secondary circulation, while the parameterisation may be attributed to the primary circulation. This model is neither intended nor capable to prove whether CISK or WISHE is closer to reality; it serves as a system for a linear normal mode or asymptotic growth analysis and, possibly, provides a step towards future WISHE and CISK comparisons. In this sense, this linear WISHE-type instability analysis lies at the simplistic side of the spectrum of model complexity. Section 2 describes the model, the solutions, and the dispersion-relation. The structures of the two modes of response are described in the subsequent sections 3 and 4. A conclusion (section 5) summarises the analysis.

## 2. Model Equations and Solutions

Following Charney and Eliassen (1964) a two-layer model in pressure coordinates is employed for inviscid, balanced disturbances of a stratified basic state at rest. The vertical geometry for the dynamical system is presented in Fig. 1. Slab-

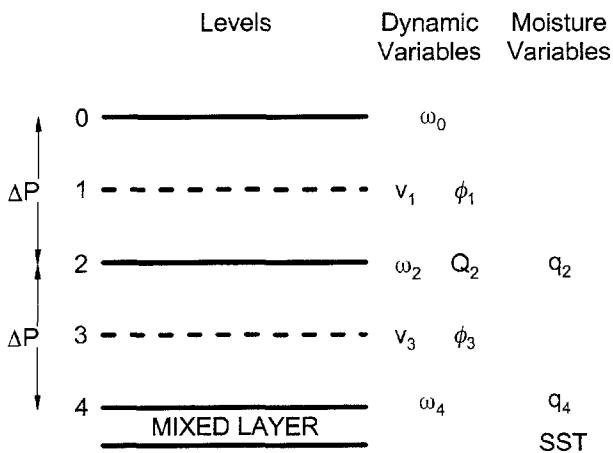


Fig. 1. The two-layer model geometry of the classical Charney and Eliassen (1964) and Mak (1981) model. See text for notations

symmetry on an  $f$ -plane simplifies the dynamic equations which, after McBride and Fraedrich (1995), are:

$$\begin{aligned}
 \sigma_u u_1 - f v_1 &= 0 & \sigma_u u_3 - f v_3 &= 0 \\
 f u_1 &= -\partial \phi_1 / \partial y & f u_3 &= -\partial \phi_3 / \partial y \\
 \partial v_1 / \partial y + (\omega_2 - \omega_0) / \Delta p &= 0 \\
 \partial v_3 / \partial y + (\omega_4 - \omega_2) / \Delta p &= 0 \\
 \omega_0 &= 0 & \omega_4 &= K \partial u_3 / \partial y \\
 -[p / R_d \Delta p] \sigma_\phi (\phi_3 - \phi_1) &= (p S / R_d) \omega_2 + Q_2 / c_p \\
 Q_2 / c_p &= \text{heating} & |y| &< b \\
 Q_2 / c_p &= 0 & |y| &> b
 \end{aligned} \tag{2.1}$$

Subscripts are attached to the growth rate,  $\sigma$ , serving as tracers to identify the origin for later simplifications. The primary circulation is characterised by the zonal balanced flow  $u$ , the secondary circulation induced by Ekman pumping represents the meridional circulation and is associated with the inverse Ekman time-scale  $E = Kf / \Delta p \sim 0.35/\text{day}$  for the Ekman layer depth  $K = 50 \text{ hPa}$ , the Coriolis parameter  $f = 0.377 \cdot 10^{-4} \text{ s}^{-1}$  and the pressure interval  $\Delta p \sim 450 \text{ hPa}$ . The associated Rossby deformation radius  $R = (\Delta p^2 S / f^2)^{1/2} \sim 1700 \text{ km}$ , used to normalise the  $y$ -coordinate, can be introduced with the constant static stability parameter,  $S \sim 2 \cdot 10^{-2} \text{ m}^2 \text{ sec}^{-2} \text{ hPa}^{-2}$ .

The diabatic heating,  $Q_2$ , occurs in an inner domain  $|y| < b$  with upward motion while adiabatic processes govern the outer region  $|y| > b$ . The formulation of the diabatic processes requires consideration of the moisture budget, before a parameterisation of the cumulus heating can be introduced in a consistent manner.

### 2.1 Moisture Budget and Cumulus Parameterisation

The moisture budget is used to derive and interpret the cumulus heating considering a vertical column with conservation of equivalent potential temperature:  $\int_0^4 Q dp = -L \int_0^4 (dq/dt) dp = Q_2 \Delta p$ . Neglecting the terms  $\int \partial q / \partial t dp$  and  $\int \mathbf{v} \cdot \nabla q dp$ , integrating by parts with moisture being carried at the middle level 2 and the boundary 4, one obtains (see McBride and

Fraedrich, 1995):

$$\begin{aligned}
Q_2 \Delta p &= -L \int (dq/dt) dp \\
&\sim -L \int \omega (\partial q / \partial p) dp \\
&\sim -L \left\{ \frac{1}{2} \omega_2 q_2 + \frac{1}{2} (\omega_4 + \omega_2) (q_4 - q_2) \right\} \\
&= -\frac{1}{2} L \{ \omega_4 q_4 (1 - q_2/q_4) + \omega_2 q_4 \}. \quad (2.2)
\end{aligned}$$

That is, cumulus heating comprises two components: (a) The first term on the right hand side,  $\omega_4 q_4 (1 - q_2/q_4)$ , can be associated with the turbulent moisture flux at the sea surface,  $\rho_s \langle w' q' \rangle_{sfc}$ , which is conveniently parameterised in terms of the primary circulation at level 3:

$$\omega_4 q_4 \sim -g \rho_s \langle w' q' \rangle_{sfc} \sim -c_t \rho_s g (q_{sfc} - q_4) |u_3| \quad (2.3)$$

with the turbulent transfer coefficient  $c_t$ . This yields  $\omega_4 q_4 (1 - q_2/q_4) \sim -\frac{1}{2} c_t \rho_s g (q_{sfc} - q_4) |u_3|$  setting  $2q_2 \sim q_4$ . A comprehensive moisture analysis requires eddy plus scaled transports including CISK-type heating. This will be discussed elsewhere. Note that  $\text{sign}(c_t) = \text{sign}(u_3)$  provides the proper sign-relation when deducing the solution of the instability problem. This is a primary circulation induced heating (or wind induced surface heat exchange, WISHE). Introduction to the thermodynamic equation leads to the WISHE-type parameterisation which is characterised by the parameter  $\delta = -(L/c_p) (1/\Delta p)^{1/2} (\omega_4 q_4) (1 - q_2/q_4) / |u_3| = \frac{1}{4} c_t \rho_s g L (q_{sfc} - q_4) / (c_p \Delta p)$ . (b) The second term in the water balance (2.2),  $\frac{1}{2} \omega_2 q_4$ , is a secondary circulation induced heating, characterised by the parameter  $\gamma = (L/c_p) (\Delta p S p / R_d)^{-1} (\frac{1}{2} \omega_2 q_4) / \omega_2 \sim 80 q_4$ :

$$\text{HEATING} \quad Q_2/c_p = \delta |u_3| - (pS/R_d) \gamma \omega_2 \quad (2.4)$$

## 2.2 Solutions

Combination of the dynamic Eqs. (2.1) with the cumulus parameterisation (2.4) and normalising the  $y$ -coordinate with the Rossby deformation radius,  $R^2 = \Delta p^2 S / f^2$ , gives

$$\begin{aligned}
\text{outer} \quad (y > |b/R|) : v_{yy} - A^2 v &= 0 \\
\text{inner} \quad (y < |b/R|) : v_{yy} + D v_y + B^2 v &= 0 \quad (2.5)
\end{aligned}$$

The evaporation-wind feedback which appears only in the  $v_y$ -term is associated with  $D$ . The external parameters,  $A$ ,  $B$ , and  $D$  are

$$\begin{aligned}
A^2 &= (2\sigma_u + E) / [\sigma_u + E] \\
B^2 &= (\sigma_\phi / \sigma_u) (2\sigma_u + E) / [(\gamma - 1)(\sigma_u + E)] \\
D &= -2W / [(\gamma - 1)(\sigma_u + E)]. \quad (2.6)
\end{aligned}$$

The following comments on the three parameters are in order:

An inverse WISHE time-scale,  $W$ , can be introduced characterising the WISHE-type heating,  $2W = (\delta/R) (R_d \Delta p / p f) \sim [c_t L (q_{sfc} - q_4) / c_p T_s] (g/f) R^{-1} \sim (10^5/\text{day}) \cdot c_t (q_{sfc} - q_4) \sim 0.50/\text{day}$  with  $c_t \sim 1.0 \cdot 10^{-3}$  and  $(q_{sfc} - q_4) \sim 5 \cdot 10^{-3}$ , where  $T_s \sim 2p / \rho_s R_d \sim 290 \text{ K}$  with  $p = 500 \text{ hPa}$ . This is a useful measure to compare cumulus heating and frictional damping characterised by the inverse Ekman time-scale,  $E = Kf / \Delta p \sim 0.35/\text{day}$ .

An estimate of the  $\gamma$ -parameter, which characterises the mid-level heating gives  $\gamma = (L/c_p) (\Delta p S p / R_d)^{-1} (\frac{1}{2} \omega_2 q_4) / \omega_2 \sim 80 q_4 \sim 1.2 > 1$ .

Realistic parameter values for the inverse Ekman and WISHE time scales are  $E \sim 0.35/\text{day}$  and  $W \sim 0.25/\text{day}$ , and the mid-level heating term is  $E(\gamma - 1)^{1/2} \sim 0.2/\text{day}$  with  $\gamma \sim 1.2$ . The condition  $\gamma = 1$  leads to the special case of a linear inner region profile,  $v_y + (B^2/D)v = 0$ .

In the inner domain one has to realise that  $\text{sign}(c_t) = \text{sign}(u_3)$  requires a sign-change in  $W$ , if an eastward or negative zonal component (associated with a southward or negative meridional wind) is to generate evaporation. This leads to  $W < 0$  and thus  $D > 0$ , and meridionally trapped perturbations.

The outer solutions are straight forward; for  $v_3$  and  $\phi_3$  one obtains:

$$\begin{aligned}
\text{OUTER} \quad v_{3o} &= -V_o \exp\{-A(|y| - b)\} \\
\phi_{3o} &= -V_o (f^2 / \sigma_u) (1/A) \\
&\quad \cdot \exp\{-A(|y| - b)\}. \quad (2.7)
\end{aligned}$$

The structure of the inner solution depends on the root,  $-\frac{1}{2} D \pm (\frac{1}{4} D^2 - B^2)^{1/2}$ , of the characteristic polynomial where the sign of  $D$  describes the damping of the inner spatial eigenmode. Two regimes may be distinguished:

(a)  $r^2 = (\frac{1}{4} D^2 - B^2) > 0$ : The WISHE-type heating,  $W$  or  $\frac{1}{4} D^2$ , dominates over the secondary

circulation influence,  $B^2$ . The spatial structure of the solution is formed by hyperbolic eigenfunctions in the inner convective area  $|y| < b$ . Realising  $\text{sign}(c_i) = \text{sign}(u_3)$  means that a southward (negative) meridional wind is associated with an eastward (negative) zonal component generating (positive) evaporation with  $W < 0$ . This provides a damped meridional structure ( $D > 0$  for  $y > 0$ , and vice versa) corresponding to meridionally trapped perturbations:

$$\begin{aligned} \text{MODE-1} \quad v_{3i} &= -V_i \exp(-\frac{1}{2}Dy) \text{sh}(ry) \\ \phi_{3i} &= +V_i f^2 / (\sigma_u B^2) \exp(-\frac{1}{2}DY) \\ &\quad \cdot \{-\frac{1}{2}D \text{sh}(ry) - r \text{ch}(ry)\} \end{aligned} \quad (2.8)$$

(b)  $r^2 = (B^2 - \frac{1}{4}D^2) > 0$ : The secondary circulation induced heating  $B^2$ , dominates over the WISHE term,  $W$  or  $\frac{1}{4}D^2$ . The spatial structure of the solutions is formed by trigonometric eigenfunctions in the inner convective area  $|y| < b$ . Again, realising that  $\text{sign}(c_i) = \text{sign}(u_3)$ , the solutions describe meridionally trapped perturbations in terms of trigonometric (and not hyperbolic) functions. Thus, for  $\gamma > 1$ , one obtains the meridional wind and the geopotential height for  $y > 0$ :

$$\begin{aligned} \text{MODE-2} \quad v_{3i} &= -V_i \exp(-\frac{1}{2}Dy) \sin(ry) \\ \phi_{3i} &= +V_i f^2 / (\sigma_u B^2) \exp(-\frac{1}{2}DY) \\ &\quad \cdot \{-\frac{1}{2}D \sin(ry) - r \cos(ry)\}. \end{aligned} \quad (2.9)$$

For brevity and reference we refer to these regimes as mode-1 and mode-2.

**PURE REGIMES:** Before analysing the stability properties of this model, the cases of pure modal regimes are discussed: (a) The special case  $\gamma = 0$  abandons the influence of the secondary circulation on cumulus heating. In this case,  $-A^2$  replaces  $B^2$  and  $D' = -2W / (\sigma_u + Kf / \Delta p) > 0$  replaces  $D$  in the inner domain. The resulting dynamical system leads to meridionally untrapped solutions which, therefore, have to be rejected as non-physical. (b) The special case  $W = 0$  emerges as a singular solution which abandons the influence of the WISHE-type heating. This case requires  $D = 0$  in the inner domain and the resulting dynamical system is identical with the special case of the ‘fast mode

without CISK mode’ discussed in McBride and Fraedrich (1995, Table 1).

### 2.3 Width-Growth Relation (Dispersion)

The kinematic and dynamic boundary conditions at  $y = \pm b$ ,  $v_{3i} = v_{3o}$  and  $\phi_{3i} = \phi_{3o}$ , lead to the width-growth (or dispersion) relation. This may be formulated in terms of the external model parameters and the time scales involved: the Ekman damping,  $E = Kf / \Delta p$ , and the WISHE-type heating,  $W$ , characterising the two inverse feedback time-scales. The dispersion or width-growth relations of the mode-1 and mode-2 regimes are:

$$\begin{aligned} \text{MODE-1} \quad (\frac{1}{4}D^2 - B^2) > 0 : \\ b/R &= (\frac{1}{4}D^2 - B^2)^{-1/2} \\ &\quad \cdot \text{Arth}\{(\frac{1}{4}D^2 - B^2)^{1/2} / (B^2/A - \frac{1}{2}D)\} \end{aligned} \quad (2.10)$$

$$\begin{aligned} \text{MODE-2} \quad (B^2 - \frac{1}{4}D^2) > 0 : \\ b/R &= (B^2 - \frac{1}{4}D^2)^{-1/2} \arctan\{(B^2 - \frac{1}{4}D^2)^{1/2} / \\ &\quad (B^2/A - \frac{1}{2}D)\}. \end{aligned}$$

Although the meridional eigenfunctions are structurally different, the dispersion relations can be treated simultaneously for both regimes realising  $\sin(x) = -\text{ish}(ix)$ ,  $\cos(x) = \text{ch}(ix)$ ,  $\tan(x) = -\text{ith}(ix)$ . The dispersion  $b/R = f(W, \sigma)$  forms a hyperplane in the  $(W, b/R, \sigma)$ -space. Three cross-sections are presented to describe the stability properties: the  $(W, b/R)$ -plane, the  $(W, \sigma)$ -plane, and the  $(b/R, \sigma)$ -plane (Fig. 2a-c).

The separatrix between both instability regimes is the intersection of the hyperplane  $\frac{1}{4}D^2 - B^2 = 0$  with the dispersion (2.10)  $b/R = f(W, \sigma)$ . The dispersion at the separatrix is obtained applying l’Hospitals’ rule. Inserting (2.6) yields  $(b/R)^* = (B^2/A - \frac{1}{2}D)$  with

$$\begin{aligned} \text{SEPARATRIX} \quad \frac{1}{4}D^2 - B^2 = 0 : \\ \sigma^* &= -\frac{3}{4}E + \{E^2/16 + \frac{1}{2}W^*/(\gamma - 1)\}^{1/2} \\ (b/R)^* &= (\sigma^* + E)(\gamma - 1) / \\ &\quad \{[(2\sigma^* + E)(\sigma^* + E)]^{1/2} - W^*\}. \end{aligned} \quad (2.11)$$

The associated  $\sigma^*$ -growth rate increases with the inverse time scale  $W^*$ . The meridional ex-

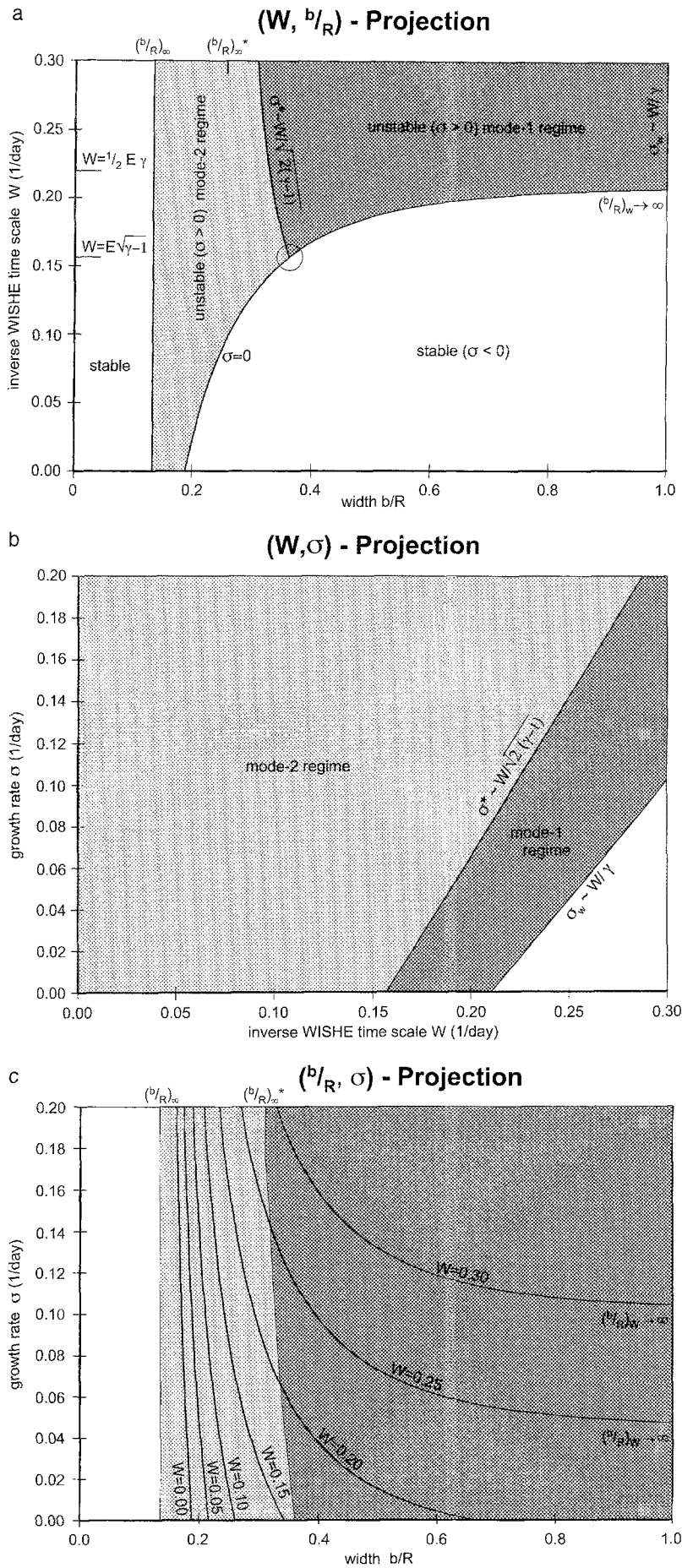


Fig. 2. Boundaries of the instability regimes of the linear slab-symmetric two layer model in the  $(W, b/R, \sigma)$ -space: (a)  $(W, b/R)$ -projection, (b)  $(W, \sigma)$ -projection, and (c)  $(b/R, \sigma)$ -projection. Tables 1 and 2 contain further details

tent  $(b/R)^* = [(\sigma^* + E)/(2\sigma^* + E)]^{1/2} \{(\gamma - 1)/[1 - (\gamma - 1)^{1/2}]\}^{1/2}$  decreases from  $(b/R)_o^* = (\gamma - 1)/\{1 - (\gamma - 1)^{1/2}\}$  at  $\sigma^* = 0$  to  $(b/R)_\infty^* = (\sqrt{\frac{1}{2}})(\gamma - 1)/\{1 - (\gamma - 1)^{1/2}\}$  for  $\sigma^* \rightarrow \infty$ . This intersection of hyperplanes separates dispersion of the mode-1 and mode-2 regimes. That is, the separatrix  $((b/R)^*, \sigma^* < \infty, W^*)$  represents the minimum growth of the regime dominated by the secondary circulation (mode-2) and the maximum growth of the mode-1 regime dominated by WISHE-type heating.

### 3. Mode-1 Regime

The mode-1 width-growth relation (2.10) dominated by the WISHE-type heating,  $(\frac{1}{4}D^2 - B^2) > 0$ , is analysed in the instability region,  $\sigma \geq 0$ . In particular, the projections onto the  $(W, b/R)$ -,  $(W, \sigma)$ -, and the  $(b/R, \sigma)$ -planes are presented for fixed  $E$  and  $1 < \gamma < 2$ , but for changing  $W$ :

$$\begin{aligned} b/R &= (\sigma + E)(\gamma - 1)/ \\ &\{W^2 - (2\sigma + E)(\sigma + E)(\gamma - 1)\}^{1/2} \\ &\cdot \text{Arth}\{[W^2 - (2\sigma + E)(\sigma + E)(\gamma - 1)]^{1/2}/ \\ &[(2\sigma + E)(\sigma + E)]^{1/2} - W\}. \end{aligned} \quad (3.1)$$

This instability regime emerges with growth-rates,  $\sigma^* \geq \sigma \geq \sigma_w$ , and related widths,  $(b/R)^* \leq (b/R) \leq (b/R)_w$ , if the inverse time scale,  $W$ , exceeds a sufficiently large intensity threshold,  $W \geq E(\gamma - 1)^{1/2} \sim 0.15$ , to overcome the dominance of the secondary circulation induced (mode-2) heating effect.

The upper bound of the growth rate,  $\sigma^*$ , coincides with the separatrix (2.11) which, in  $(W, b/R, \sigma)$ -space, changes with increasing the inverse time scale,  $W$ : The instability domain opens at the bifurcation point  $(W, b/R, \sigma)_o^* = (E(\gamma - 1)^{1/2}, (\gamma - 1)/\{1 - (\gamma - 1)^{1/2}\}, 0)$ . For infinitely large inverse time scale,  $W$ , the maximum growth rate and its width are attained at the following parameter constellation:  $(W, b/R, \sigma)_\infty^* = (\infty, (\sqrt{\frac{1}{2}})(\gamma - 1)/\{1 - (\gamma - 1)^{1/2}\}, \infty) \sim (\infty, 0.26, \infty)$ . Any additional intermediate locus,  $(W, b/R, \sigma)^*$ , as for example at  $W = \frac{1}{2}E\gamma$  may be computed, substituting  $W$  and  $b/R$  into the width-growth relation (2.11) of the separatrix.

The two lower  $\sigma$ -bounds of the instability domain attain a zero *and* finite (minimum) growth rate,  $\sigma_w = 0$  and  $> 0$ . Accordingly, the

associated width is finite,  $\infty > (b/R)_w > 0$ , and has infinitely large values,  $(b/R)_w \rightarrow \infty$  (Fig. 2c):

lower bound ( $\sigma_w = 0$ ):

$$\begin{aligned} (b/R)_w &= E(\gamma - 1)/\{W^2 - E^2(\gamma - 1)\}^{1/2} \\ &\text{Arth}\{[W^2 - E^2(\gamma - 1)]^{1/2}/(E - W)\} \end{aligned}$$

This zero- or ( $\sigma_w = 0$ )-bound occurs for  $\frac{1}{2}E\gamma \geq W \geq E(\gamma - 1)^{1/2}$  satisfying  $W^2 - (2\sigma + E)(\sigma + E)(\gamma - 1) \geq 0$ . The associated width  $(b/R)_w$  increases with increasing inverse time scale  $W$ . In the  $(W, b/R, \sigma)$ -space this domain commences at  $(W, b/R, \sigma)_w = (E(\gamma - 1)^{1/2}, (\gamma - 1)/\{1 - (\gamma - 1)^{1/2}\}, 0) \sim (0.15, 0.36, 0)$  and ends at  $(W, b/R, \sigma)_w = (\frac{1}{2}E\gamma, \infty, 0) \sim (0.21, \infty, 0)$ . Further increase of the inverse WISHE time scale,  $W \geq \frac{1}{2}E\gamma \sim 0.21$ , creates a finite *minimum growth rate*,  $W_w^2 - \frac{1}{2}\gamma\{(2\sigma_w + E)(\sigma_w + E)\}^{1/2} = 0$ , as a lower ( $\sigma_w > 0$ )-bound (Fig. 2b):

lower bound ( $\sigma_w > 0$ ):

$$\begin{aligned} \sigma_w &= -\frac{3}{4}E + \{E^2/16 + W_w^2/\gamma^2\}^{1/2} \geq 0 \\ &\text{with } (b/R)_w \rightarrow \infty. \end{aligned}$$

The meridional width is infinitely large,  $(b/R)_w \rightarrow \infty$ , because the argument of  $\text{Arth}(X \rightarrow 1) \rightarrow \infty$ ; the denominator of  $X = Z/N, N = (2\sigma + E)(\sigma + E) - W^2 \geq 0$ , guarantees positive  $b/R$ -values.

The mode-1 instability structure in  $(W, b/R, \sigma)$ -space is summarised in Table 1: For  $W \geq E(\gamma - 1)^{1/2}$  and  $1 < \gamma \leq 2$ , the mode-1 instability regime is dominated by the WISHE-type heating. This regime commences once the inverse time scale exceeds the threshold,  $W = E(\gamma - 1)^{1/2}$ , which depends both on the magnitude of Ekman damping,  $E$ , and the heating induced by the secondary circulation,  $1 < \gamma < 2$ . The meridional width range,  $b/R$ , is finite and limited by the zero growth bound ( $\sigma = 0$ ) in the interval  $E(\gamma - 1)^{1/2} < W < \frac{1}{2}E\gamma$  and the upper bound  $\sigma^*$ . Further enhancement of the WISHE influence,  $W \geq \frac{1}{2}E\gamma$ , leads to finite (though relatively small) minimum growth rates effecting infinitely large space scales,  $(b/W)_w$  (Fig. 2c). At  $\gamma = 2$ , however, the mode-1 regime vanishes; both  $\text{Arth}(X \rightarrow 1) \rightarrow \infty$  and  $\text{Arth}(X = 0)$  occur simultaneously satisfying  $W = \frac{1}{2}E\gamma$  and  $W = E(\gamma - 1)^{1/2}$ ; that is  $\sigma_w = \sigma^*$  (Fig. 2b). Thus, for  $\gamma > 2$ , the mode-1 structure disappears and the instability is taken over by the mode-2 regime

Table 1. *Mode-1 Instability Regime in  $(W, b/R, \sigma)$ -space for  $1 < \gamma \leq 2$* 

Parameter domain	Growth rates	Width ranges
$W = E(\gamma - 1)^{1/2}$	$0 = \sigma = \sigma^*$	$(b/R)_o^* = (\gamma - 1)/\{1 - (\gamma - 1)^{1/2}\}$
$E(\gamma - 1)^{1/2} \leq W \leq 1/2E\gamma$	$0 \leq \sigma \leq \sigma^*$ $\sigma^* = -\frac{3}{4}E + [E^2/16 + \frac{1}{2}W^2/(\gamma - 1)]^{1/2}$	$\infty \geq (b/R)_{wo} \geq b/R \geq (b/R)^*$
$W > \frac{1}{2}E\gamma$	$0 < \sigma_w \leq \sigma \leq \sigma^*$ $\sigma_w = -\frac{3}{4}E + [E^2/16 + w^2/\gamma^2]^{1/2} < \sigma^*$	$(b/R)_w \rightarrow \infty$
$W \rightarrow \infty$	$\sigma^* \rightarrow \infty$	$(b/R)_\infty^* = \sqrt{\frac{1}{2}}(\gamma - 1)/\{1 - (\gamma - 1)^{1/2}\}$

(dominated by the midlevel massflux term) independent of the magnitude of the WISHE contribution  $W$  (dominating in the mode-1 regime). Figure 3a shows the amplitude profiles of the meridional wind and the geopotential height at the lowest level 3.

#### 4. Mode-2 Regime

The mode-2 width-growth relation (2.10) of the secondary circulation dominated heating,  $(B^2 - \frac{1}{4}D^2) < 0$ , related to the mid-level vertical massflux, is analysed in its instability region,  $\sigma \geq 0$ . In particular, the projections onto the  $(W, b/R)$ -,  $(W, \sigma)$ -, and the  $(b/R, \sigma)$ -planes are presented for fixed  $E$  and  $1 < \gamma < 2$ , and changing  $W$ :

$$b/R = (\sigma + E)(\gamma - 1) / \{ (2\sigma + E)(\sigma + E)(\gamma - 1) - W^2 \}^{1/2} \cdot \arctan\{ [(2\sigma + E)(\sigma + E)(\gamma - 1) - W^2]^{1/2} / [(2\sigma + E)(\sigma + E)]^{1/2} - W \}. \quad (4.1)$$

The function  $\arctan\{x\}$  covers the interval  $0 < x < \infty$ , which guarantees positive width scales,  $b/R > 0$  for  $y > 0$ . As in the mode-1 case there is an upper  $\sigma$ -bound and a zero or finite lower  $\sigma$ -bound limiting the width or  $(b/R)$ -interval of the mode-2 regime (Fig. 2a).

The upper  $\sigma$ -bound is defined by an infinitely large *maximum growth*  $\sigma = \infty$ ; the corresponding width,  $(b/R)_\infty$ , is finite and can directly be deduced from (4.1):

upper bound ( $\sigma = \infty$ ):

$$(b/R)_\infty = [\frac{1}{2}(\gamma - 1)]^{1/2} \arctan(\gamma - 1)^{1/2}.$$

In the parameter space (Fig. 2c) this bound is a constant independent of the inverse time scales  $W$  and  $E$ ,  $(W, b/R, \sigma)_\infty = (W, [\frac{1}{2}(\gamma - 1)]^{1/2} \arctan(\gamma - 1)^{1/2}, \infty)$ ; it coincides with the fast mode solution of McBride and Fraedrich (1995). For  $1 < \gamma < 2$ , the  $(b/R)_\infty$ -range spans  $0 < (b/R)_\infty < (\sqrt{\frac{1}{2}})\arctan(1)$ .

There are two types of lower  $\sigma$ -bounds: Zero growth,  $\sigma = 0$ , is the minimum growth of the mode-2 regime and observed in the parameter regime,  $0 \leq W \leq E(\gamma - 1)^{1/2}$ . The associated meridional extent  $(b/R)_o$  increases with the inverse time scale  $W$  (Fig. 2a):

lower bound ( $\sigma = 0$ )

$$(b/R)_o = E(\gamma - 1) / \{ E^2(\gamma - 1) - W^2 \}^{1/2} \cdot \arctan\{ [E^2(\gamma - 1) - W^2]^{1/2} / (E - W) \}.$$

In  $(W, b/R, \sigma = 0)$ -space, there is a lower and an upper  $W$ -limit associated with  $(\sigma = 0)$ -growth. The lower  $W$ -bound,  $W = 0$ , is related to the instability modes discussed in McBride and Fraedrich (1995) which occurs at  $(W, b/R, \sigma)_o = (0, (\gamma - 1)^{1/2} \arctan(\gamma - 1)^{1/2}, 0) \sim (0, M, 0)$ . The upper  $W$ -bound for zero-growth can be derived by applying l'Hospital's rule to (4.1):  $(b/R)_o \rightarrow E(\gamma - 1)/(E - W) : (W, b/R, \sigma)_o = (\frac{1}{2}E\gamma, (\gamma - 1)/(1 - \frac{1}{2}\gamma), 0) \sim (0.21, 0.5, 0)$ . This point,  $W = E(\gamma - 1)^{1/2}$ , lies on the separatrix between both mode-1 and -2 regimes. It represents the bifurcation point at which, with increasing  $W \geq E(\gamma - 1)^{1/2}$ , the mode-1 regime opens with the width-scale  $(b/R)_o^* = (\gamma - 1)/[1 - (\gamma - 1)^{1/2}]$ .

The other lower  $\sigma$ -bound is finite; it corresponds with the separatrix  $\sigma^*$ , and represents the minimum growth limit of the mode-2 regime. With growing influence of the WISHE

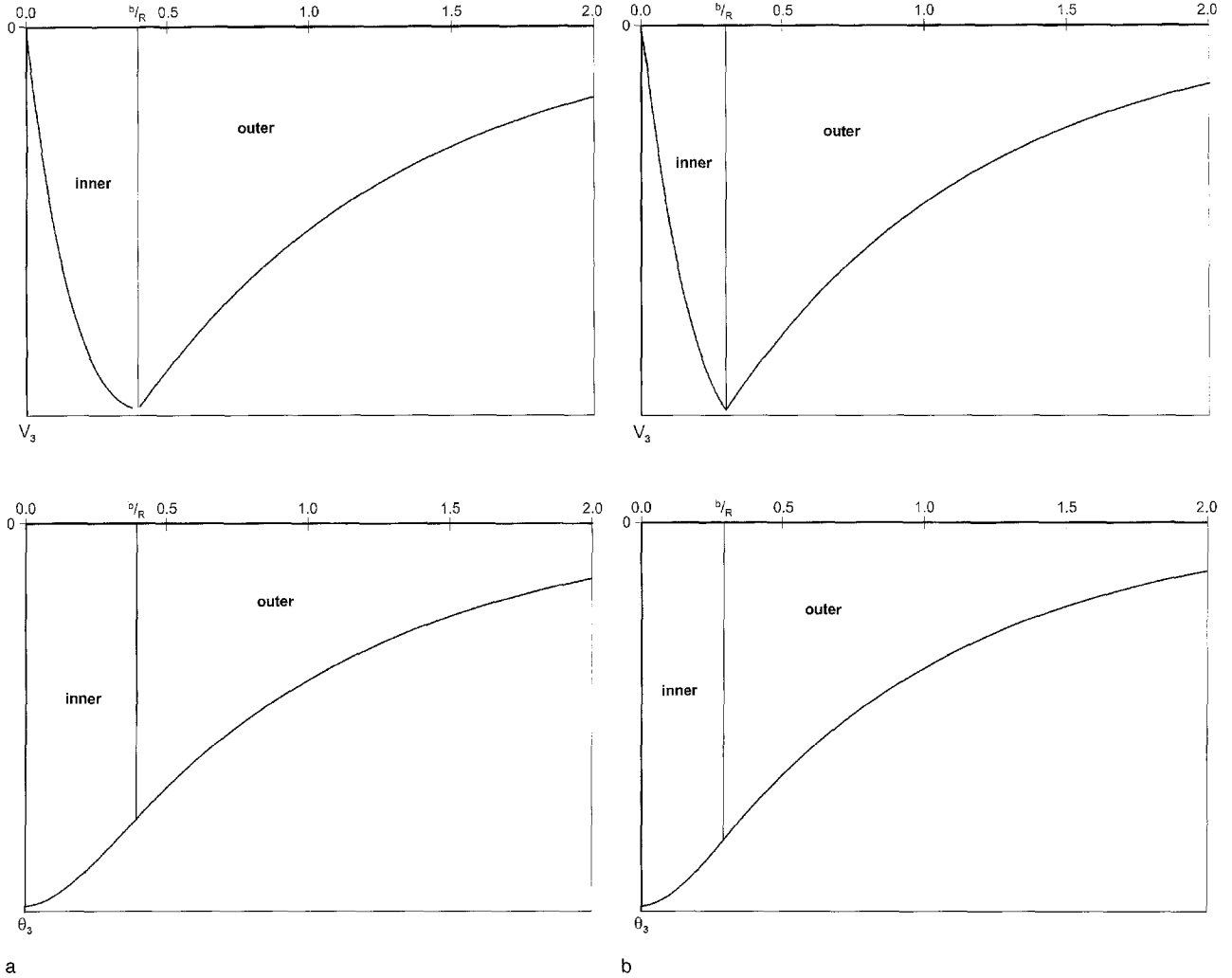


Fig. 3. Amplitude structure of the disturbances: (a) Mode-1 instability regime with hyperbolic function in the inner domain ( $W = 0.2/\text{day}$ ,  $b/R = 0.4$ ); (b) Mode-2 instability regime with trigonometric functions in the inner domain ( $W = 0.2/\text{day}$ ,  $b/R = 0.3$ )

Table 2. Mode-2 Instability Regime in  $(W, b/R, \sigma)$ -space

Parameter domain	Growth rates	Width ranges
$W = 0$	$0 \leq \sigma < \infty$	$(b/R)_o \geq b/R \geq (b/R)_\infty$
$0 < W < E(\gamma - 1)^{1/2}$	$0 \leq \sigma < \infty$ with	$(b/R)_o \geq b/R \geq (b/R)_\infty$ $(b/R)_o = (\gamma - 1)^{1/2} \arctan(\gamma - 1)^{1/2}$ $(b/R)_\infty = (\sqrt{1/2})(\gamma - 1)^{1/2} \arctan(\gamma - 1)^{1/2}$
$W = E(\gamma - 1)^{1/2}$	$\sigma^* \leq \sigma < \infty$	$(b/R)_o^* = (\gamma - 1) / \{1 - (\gamma - 1)^{1/2}\} < (b/R)_\infty$
$W > E(\gamma - 1)^{1/2}$	$\sigma^* \leq \sigma < \infty$	$(b/R)^* \geq b/R \geq (b/R)_\infty$

type heating,  $W$ , this lower bound emerges at the bifurcation point,  $W = E(\gamma - 1)^{1/2}$ , and remains on the separatrix between of the regimes (see above). Note that in the limit of large  $W$  (and  $\sigma$ ), there is a remaining width span,

$(b/R)_\infty < (b/R)_\infty^*$ , for the mode-2 regime. The results are summarised in Table 2. Figure 3b shows the amplitude profiles of the meridional wind and the geopotential height at the lowest level 3.

## 5. Summary and Discussion

Wind induced sensible heat exchange (WISHE) is adopted as a parameterisation of cumulus heating. It is used to replace the CISK-type heating in the classical Charney-Eliassen (1964) model satisfying the associated water budget of the system. Two instability regimes emerge with formally different spatial amplitude structures. The mode-1 instability regime is dominated by WISHE type heating; the mode-2 is dominated by the secondary circulation induced heating. WISHE related instabilities reveal the following results deduced from the appropriate dispersion relation.

(i) The mode-1 instability regime requires sufficient intensity of the surface heat exchange to obtain finite growth rates within a finite scale range. Beyond a certain intensity threshold of the heating parameter, however, the scale range extends to infinitely large values. The maximum growth rates, though relatively small, occur at the smaller scale limit (and vice versa), which separates mode-1 and mode-2 regimes. (ii) The mode-2 instability regime joins mode-1 at its large growth (and small scale) boundary and extends towards infinitely large growth rates at smaller but finite scales.

Both regimes comprise the wide spectrum of space and time scales as they can be observed in the tropical convective complexes, ranging from the cloud cluster scale to the Madden-Julian oscillation. Dominance of the wind induced surface heat exchange influences the larger scale processes associated with smaller growth rates whereas, for smaller scales, the secondary circulation induced heating in mid-levels dominates with the large growth rates.

Re-interpreting the CISK heating (proportional to the Ekman pumping of the secondary circulation) in the classical Charney-Eliassen (1964) model such that it also satisfies the associated water budget (McBride and Fraedrich, 1995) reveals the following features. There are two regimes associated with CISK: The relatively fast mode is similar to the mode-2 above, with an infinite growth rate at a minimum finite scale. The slow (or classical CISK) mode, however, shows the well known features of finite maximum growth at vanishingly small spatial scales. Both modes attain a zero growth limit at

finite scales so that model instability occurs in a finite width span. That is, replacing the CISK-type parameterisation by a WISHE-type extends the scale range effected by cumulus heating to larger scales *and* retains the fast mode features at the smaller but finite scales, which are associated with the secondary circulation induced midlevel heating.

### Acknowledgements

Part of this paper is sponsored by the Max-Planck Prize; discussions with John McBride, Bureau of Meteorology Research Centre (Melbourne), colleagues from the University of New South Wales (Sydney), R. Blender (Hamburg) and L. Schade (München) are appreciated. The professional drawing assistance by Ms. M. Grunert is gratefully acknowledged.

### List of Symbols

#### *a) Dynamic Variables, Model Parameters and Geometry*

$u, v, \omega, \phi$	zonal, meridional velocity, vertical p-velocity, geopotential
$Q, c_p, R_d, L$	heating, specific heat, gas constant, latent heat
$f, S$	Coriolis parameter, static stability
$y$ and $p, b, \Delta p, K$	meridional and vertical axes, lateral width of area with convective heating, vertical differences, Ekman layer depth
$i, o$	subscripts: inner and outer domain
$\sigma, \sigma_u, \sigma_\phi$	growth rate with trace parameters

#### *b) Feedback and Derived Parameters, Functions, Subscripts, and other Parameters*

$q, T, \rho, R$	humidity, temperature, density, Rossby deformation radius
$\delta; \gamma$	feedback: evaporation-wind; midlevel heating – massflux
$L\rho_s \langle w'q' \rangle_{sf}, c_t$	surface evaporation, turbulent transfer coefficient
$A, B, D, E, W, r$ $\sin, \text{sh}; \arctan, \text{Arth}$	see text for parameter combinations trigonometric, hyperbolic functions; their inverses
$*, \sigma^*, (b/R)^*$	separatrix; values for growth rate and normalised width
$\sigma_w, (b/R)_w$	separation between mode-1 and mode-2 regimes; further subscripts, 0 or $\infty$ , indicate the magnitude of the growth rate.
$()_{0..4}; ()_y; ()_s; V_o$	layer, partial derivative, initial value, surface or saturation.

### References

Charney, J. G., Eliassen, A., 1964: On the growth on the hurrican depression. *J. Atmos. Sci.*, **21**, 68–75.

- Mak, M., 1981: An inquiry on the nature of CISK, Part I. *Tellus*, **33**, 531–537.
- McBride, J. L., Fraedrich, K., 1995: CISK: A theory for the response of tropical convective complexes to variations in sea surface temperature. *Quart. J. Roy. Meteor. Soc.*, **121**, 783–796.
- Ooyama, K. V., 1997: Footnotes to ‘conceptual evolution’. 22nd Conference on Hurricanes and Tropical Meteorology. American Meteorological Society, May 19–23, 1997, Ft. Collins, Colorado, 13–18.
- Riehl, H., 1954: *Tropical Meteorology*. New York: McGraw-Hill, 392 pp.
- Yano, J.-I., Emanuel, K. A., 1991: An improved WISHE model of the equatorial atmosphere and its coupling with the stratosphere. *J. Atmos. Sci.*, **48**, 377–389.

Author’s address: Klaus Fraedrich, Meteorologisches Institut, Universität Hamburg, Bundesstrasse 55, D-20146 Hamburg, Germany.